

Fully differential rates for femtosecond multiphoton double ionization of neon

D. Zeidler^a, M. Weckenbrock^b, A. Staudte^b, Th. Weber^b, M. Schöffler^b, M. Meckel^b, S. Kammer^b, M. Smolarski^b, O. Jagutzki^b, V.R. Bhardwaj^a, D.M. Rayner^a, D.M. Villeneuve^a, P.B. Corkum^a, and R. Dörner^b

^a National Research Council, 100 Sussex Drive, Ottawa, Ontario, Canada K1A 0R6

^b Universität Frankfurt, D-60486 Frankfurt, Germany

ABSTRACT

We have investigated the full three-dimensional momentum correlation between the electrons emitted from strong field double ionization of neon when the recollision energy is of the order of the ionization potential. The momentum correlation in the direction perpendicular to the laser field depends on the time difference between the two electrons leaving the ion. Our results are consistent with double ionization proceeding through transient double excited states that field ionize.

Keywords: Multiphoton ionization of atoms, electron correlation, femtosecond laser

1. INTRODUCTION

When two electrons are ejected from an atom by absorption of one or more photons, correlations between the electrons are fundamental to understanding of few-body dynamics. In the single photon limit, the situation is very satisfactory today: Experiments, on one side, have yielded high accuracy fully differential cross sections from 100 meV^1 to 450 eV^2 above threshold (see^{3,4} for recent reviews). Theory, on the other, reproduces the experimental data very well.⁵⁻⁸

For the case of multiphoton absorption in ultrashort Ti:Sa laser pulses with pulse durations of below 100 fs and intensities in the 10^{14} W/cm^2 range, the situation is different: Experiments have not reached the level of sophistication as in the single photon case. Consequently, no fully differential cross sections are available yet. Theory likewise has difficulties to make reliable fully differential predictions.^{9,10} A full characterization of the system requires the determination of the three momentum components of both electrons or of one of the electrons and the ion. All experiments reported so far have left at least one momentum component unobserved.

Measurements have advanced from the observation of total double ionization rates¹¹ over ion momenta,^{12,13} single electron energy¹⁴⁻¹⁶ and angular distributions¹⁶ to the correlation between the momentum components either parallel^{17,18} or perpendicular¹⁹ to the laser field have been measured gradually. Major features, like the double hump structure in the ion momenta and the correlation in the electron momenta parallel to the field, have been reproduced by various quantum and classical calculations.²⁰

The physical mechanism responsible for these primary features is double ionization via rescattering^{21,22}: The first electron is set free by the field, accumulates energy during about half a laser cycle and is driven back to its parent ion where it can reemit a second electron. This may happen either via a direct or laser-assisted²³ electron impact ionization²² or via the creation of an intermediate excited ionic state which is later field ionized.¹⁸

In this paper, which is a follow-up of experiments and ideas shown just recently,²⁴ we report on an experiment where all kinematical observables, i.e. the full three-dimensional vector momenta of both electrons have been determined. This allows us to obtain the parallel and perpendicular momentum correlation and obtain fully differential angular distributions which is the most detailed view at the process.

Further author information: (Send correspondence to R.D.)

R.D.: E-mail: Doerner@ikf.uni-frankfurt.de, Telephone: +49 69 798 24-218

P.B.C.: E-mail: Paul.Corkum@nrc.ca, Telephone: +1 (613) 993 7390

We find three surprising results for recollision electrons near threshold: (1) The electrons have little excess momentum perpendicular to the laser field, which is comparable to that of single ionization.²⁵ (2) The two electrons are likely to possess similar momentum parallel to the laser field. (3) Electrons with similar longitudinal momentum (i.e. along the laser field) show repulsion in the perpendicular directions, whereas electrons with different momentum do not. Assuming that the momentum parallel to the laser field originates primarily from the laser field, we deduce that both electrons are emitted about 30° from the maximum of the laser field during one quadrant of the field.

These observations are consistent with doubly excited states being formed by the recolliding electron that live for a fraction of a laser period and then ionize near the maximum of the laser field.^{26,27}

2. EXPERIMENT

The experiment was performed using Cold Target Recoil Ion Momentum Spectroscopy (COLTRIMS).^{28,29} Ti:Sa laser pulses (40 fs, 800 nm, $3.9 \mu\text{J}$, 30kHz repetition rate) were focused into a supersonic Neon gas jet. The peak intensity was determined by means of three independent methods: The momentum distribution of singly charged ions in linearly polarized light was compared to ADK calculations. Second, the width of our doubly charged ion momentum distribution was compared with the value expected from.³⁰ Finally, we used circularly polarized light to determine the intensity from the electron momentum distribution of Argon single ionization. All methods consistently retrieve an intensity of $(1.9 \pm 0.3) \times 10^{14} \text{ W/cm}^2$.

Ions and electrons created in the focus are guided by a 3.9 V/cm electric and a 10.8 Gauss magnetic field towards two large area channel plate detectors with delay line position encoding.³¹ The internal temperature of the gas jet, which determines the momentum resolution for the ion momentum measurement, is lower perpendicular than parallel to its propagation direction. We chose the laser polarization parallel to the gas jet, ensuring that very small momenta perpendicular to the laser polarization are measured with sufficient resolution. The momentum resolution was monitored simultaneously in the single ionization channel where ion and electron momenta have to compensate. We achieve a momentum resolution of ± 0.035 a.u. along the spectrometer axis, ± 0.15 a.u. perpendicular and ± 0.325 a.u. parallel to the laser polarization. The last value is the resolution along the jet direction; it is governed by the jet temperature. The setting of electric and magnetic field yielded 4π solid angle for electrons up to 35 eV. The momentum of the second electron was calculated by taking the difference of the momentum of the first electron and that of the ion.

The electron count rate was 0.1; the ion rate 0.02 per shot. For single ionization, real coincidences are identified by momentum conservation between ion and electron.¹⁷ The fraction of false coincidences in which the registered ion and electron result from two different atoms both ionized in the same shot was monitored in the single ionization channel to be 9 %.

3. RESULTS

3.1. Field-aided double ionization near threshold

A laser intensity of $1.9 \times 10^{14} \text{ W/cm}^2$ corresponds to a ponderomotive energy $U_p = 11.3 \pm 2 \text{ eV}$ *. The simplest recollision picture yields a maximum return energy of the rescattered electron of $3.17U_p \approx 36 \pm 6 \text{ eV}$. It has to be considered that the electron becomes classically free at a certain distance from the ion core. Upon recollision with the core, the electron gains an additional $\sim 5 \text{ eV}$ in the laser field,³² which gives a total of $41 \pm 6 \text{ eV}$. This has to be compared to the field-free ionization potential of 41 eV for the Ne^+ ion and the lowest excitation energy of 27 eV for the first excited state of Ne^+ .

With the recollision energy being close to the threshold for non-sequential double ionization, the influence of the time dependent laser field on the instantaneous ionization potential of the parent ion³⁰ has to be taken into account. Assuming a cosine electric field $E(t) = E_o \cos \omega t$ where we neglect the time dependence of the pulse

*ponderomotive potential in SI units: $U_p = \frac{I \cdot e^2}{2\epsilon_o \cdot c \cdot m_e \omega^2}$

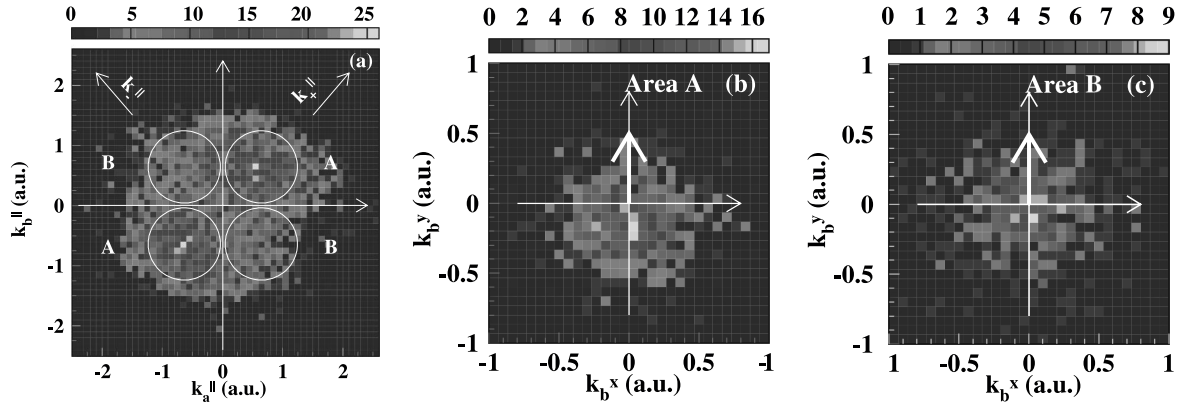


Figure 1. (a) Horizontal axis: momentum of electron a parallel to the polarization direction, vertical axis: momentum of electron b parallel to the polarization direction. The circles indicate the the region wherein events have been selected in panel b) and c). (b) Momentum components of electron b in the plane perpendicular to the polarization, the perpendicular momentum of electron a is along the positive y axis as shown by the arrow. Only events within region A have been selected. (c) same as (b) but for events in region B.

envelope E_o , the superposition of the laser electric field and a simplified hydrogen-like binding potential is given by

$$V(z, r, \theta, t) = -\frac{Z}{\sqrt{z^2 + r^2}} - E(t) \cdot z \quad (1)$$

in cylindrical coordinates (z, r, θ) , with Z being the charge state of the ion. Obviously, the ionization barrier depends on space and time: Each half laser cycle, it minimizes along the laser polarization direction $r = 0$. Electrons that escape from the core must travel through this funnel. For our laser parameters of 1.9×10^{14} W/cm² maximum intensity, corresponding to 3.8×10^{10} V/m, and $Z = 2$, the instantaneous ionization potential can decrease by as much as 21 eV from the unperturbed value.²⁷

Figure 1(a) shows the momentum correlation in the direction parallel to the laser field. The horizontal axis shows the momentum component $k_a^||$ of one electron, the vertical axis the component $k_b^||$ of the second electron. We find a maximum for both electrons ejected to the same side with similar momentum, which is in agreement with earlier measurements.^{17, 18, 30}

The recollision model gives these longitudinal momenta a simple physical explanation: They give information about the time when the electrons are ejected and the time difference between the reemission of the two electrons. Assuming that (a) the reemitted electrons leave the atom with no significant energy and (b) electron-electron momentum exchange in the final state is negligible, the parallel momentum $k_{a,b}^||$ of each electron results exclusively from the acceleration in the optical field:

$$k_{a,b}^|| = 2\sqrt{U_p} \sin \omega t_{ion} \quad (2)$$

For events with $k_a^|| \approx k_b^||$ near the diagonal $k_+^|| = k_a^|| + k_b^||$, both electrons were ejected simultaneously modulo the laser period, i.e. any time where $\sin \omega t_{ion}$ possesses the given value. The momentum difference $k_-^|| = k_a^|| - k_b^||$ along the second diagonal is related to the time difference between the ejection of the two electrons. The maximum at $k_a^|| = k_b^|| = 0.65$ a.u. then corresponds to a recollision phase ωt_{rec} of 30° off the field maximum.

3.2. Final state repulsion

Events in quadrants two and four (region B) are consistent with electrons that leave the ion at significantly different times.¹⁸ This would exclude final state interaction. Figure 1 (c) shows the momentum component of one electron in the plane perpendicular to the polarization for events indicated in region B in figure 1(a). The transverse momentum of the other electron defines the positive y axis of this graph as indicated by an arrow. The momentum distribution in Fig. 1(c) is approximately Gaussian with a $1/e$ width of 0.3 a.u. in both directions.

The width of the lateral momentum distribution is very close to what we measure for tunnel ionization in a comparable field.²⁵ The lateral electron momentum distribution is governed by the spatial width of the barrier (eq. 1) and is the minimum allowed by the uncertainty principle. The electrons therefore do not retain any angular momenta that they might have had before escaping, and we have good reasons to also expect their longitudinal excess momenta to be small (assumption a). Our observations of a loss of repulsion in region B supports an argument by Feuerstein *et al.*¹⁸ that these events are created by recollision with electron impact excitation followed by a time-delayed field ionization of the excited state.

In contrast, final state interaction is evident for electrons in region A. Fig 1(b) shows that the momentum distribution of the second electron is biased in the opposite direction to the first electron. The offset is 0.1 a.u., but the width of the distribution is approximately the same as in Fig 1(c). This result is consistent with electron repulsion in the final state,¹⁹ when electrons are emitted almost simultaneously.

Although we measure evidence that the electrons interact in their final state, the momentum transferred by the interaction is too small to make eq. 2 invalid. Using eq. 2, $k_a^{\parallel} = k_b^{\parallel} = 0.65$ a.u. implies a reemission phase ωt_{ion} of 30° off the field maximum. The observed repulsion shows that the electrons must be reemitted within a relatively small time window within the same field quadrant. This removes part of the $\sin \omega t_{ion}$ ambiguity in eq. 2.

The observation for region A is consistent with the electrons being stored in double excited states between the time of recollision and the time the laser field increases sufficiently for them to escape over the barrier. The essential role of double excited states in threshold double ionization has been previously proposed.^{26,27}

4. DIFFERENTIAL CROSS SECTIONS

Figures 2(b) and (d) show fully differential cross sections, i.e., they are not integrated over any of the observables. The sum energy of both electrons has been constrained to $10 \text{ eV} < (E_a + E_b) < 24 \text{ eV}$ and the polar emission angle θ_a of one electron (indicated by the arrow in the figures) with respect to the polarization. In addition, the figures show the coplanar geometry. That is, the azimuthal angles $\phi_{a,b}$ are fixed to confine both electrons to the plane of the figure.

Figures 2(a) and (c) show the angular distribution of electrons with different energy sharing, $E_{b,rel} = E_b/(E_a + E_b)$. The electrons are driven by the field into narrow cones along the polarization axis. For the asymmetric energy sharing, some flux is also seen in the perpendicular direction, while for the equal energy sharing there is almost a node¹⁶ at $\theta_b = 90^\circ$. If now the direction and energy of the second electron is fixed (figure 2(b)), we observe a double lobe structure with significantly more intensity for both electrons being ejected to the same side than to opposite sides. The main lobe clearly shows the influence of electron repulsion. The smaller lobe to the left side is almost symmetric. This is in accordance with our above interpretation that the emitted electrons are time delayed and hence these electrons do not see the repulsion. For unequal energy sharing (figure 2(d)), the asymmetry between the two lobes is reduced, and a significant flux is seen not only in the narrow cone along the polarization axis, but also perpendicular to it.

The narrow angular distribution along the polarization axis in all cases strikingly demonstrates the dominating influence of the laser field on the electron dynamics. It also shows that much of the final detected energy is picked up from the field after the recollision. As a consequence, the simultaneous emission of the two electrons by the recollision-ionization process leads to the main lobe pointing in the same direction as the first electron. Unlike the case of single photon double ionization,³ electron repulsion does not lead to a preferred backward emission but only to a slight bend of the main lobe.

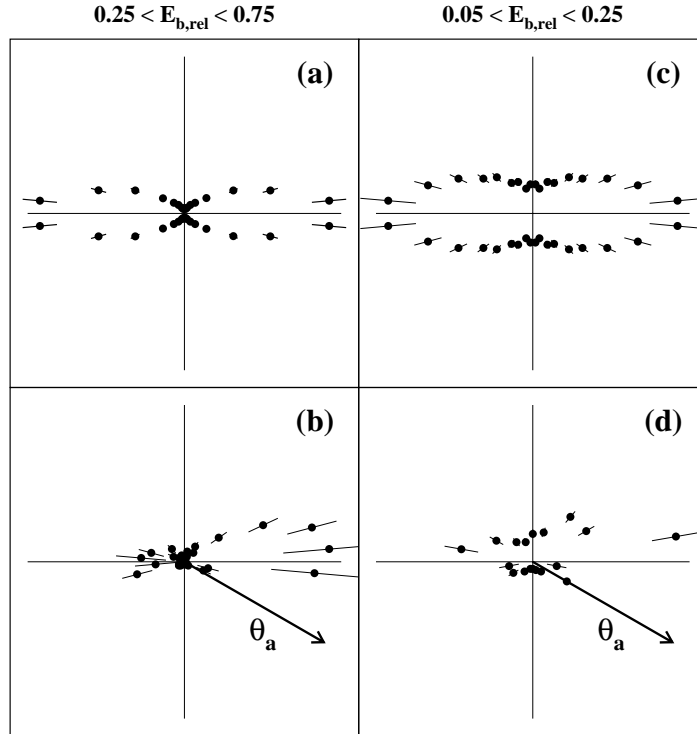


Figure 2. Angular distribution of electron b. The polarization axis is horizontal, $10 \text{ eV} < (E_a + E_b) < 24 \text{ eV}$. (a): all electrons with an energy sharing $0.25 < E_{b,rel} < 0.75$ (see text). Integrated over all angles and energies of electron a, (b): as (a) but for a fixed polar angle $\theta_a = 30^\circ \pm 10^\circ$ of electron a. Both electrons are coplanar (azimuthal angle $(\phi_a - \phi_b) < 0^\circ \pm 40^\circ$ lower half and $(\phi_a - \phi_b) < 180^\circ \pm 40^\circ$ upper half). Shown is the differential rate $d\sigma^4/dE_1 dE_2 d\Omega_a d\Omega_b$. (c) and (d): corresponding data to (a) and (b) but for an energy sharing of $0.05 < E_{b,rel} < 0.25$

5. CONCLUSIONS

The predominant role of the laser field along its direction leads to both electrons rather being observed in the same direction in the strong field case. Back-to-back emission occurs in the direction perpendicular to the laser field.

The low lateral momentum of the electron implies that the longitudinal momentum when they are reemitted from the atom is also low. Therefore, eq. 2 is applicable to both electrons independently, and so the time difference between the emission of the two electrons is resolvable up to the multi-valued nature of $\sin \omega t_{ion}$ by measuring the longitudinal momentum of both electrons. Since the lateral momentum can be used to remove the $\sin \omega t_{ion}$ ambiguity, the path is now clear for resolving the dynamics of threshold double ionization with much better than 1/4 laser cycle (attosecond) precision.

As a first step in this direction, we have performed an analogous experiment in helium at three different intensities. A glance at eqn. 1 tells that the size of the funnel through which the electrons have to escape as well as the time it is open changes with the maximum intensity of the laser field. This, in turn, should influence the amount of electron repulsion in the lateral direction.

ACKNOWLEDGMENTS

We are indebted to Horst Schmidt-Böcking and Achim Czasch for indispensable support in this project and to Andreas Becker and Robert Moshhammer for valuable discussions. The experimental work is supported by the

NRC HGF science & technology fund, DFG and BMBF (Internationales Büro). A.S. thanks the Studienstiftung des deutschen Volkes for support. Th. W. thanks Graduiertenförderung des Landes Hessen, and Th.W. and D.Z. thank the Alexander von Humboldt Stiftung for financial support.

REFERENCES

1. A. Huetz and J. Mazeau *Phys. Rev. Lett.* **85**, p. 530, 2000.
2. A. Knapp, A. Kheifets, I. Bray, T. Weber, A. L. Landers, S. Schössler, T. Jahnke, J. Nickles, S. Kammer, O. Jagutzki, L. P. Schmidt, T. Osipov, J. Rösch, M. H. Prior, H. Schmidt-Böcking, C. L. Cocke, and R. Dörner *Phys. Rev. Lett.* **89**, p. 033004, 2002.
3. J. Briggs and V. Schmidt *J. Phys.* **33**, p. R1, 2000.
4. R. Dörner, H. Schmidt-Böcking, T. Weber, T. Jahnke, M. Schöffler, A. Knapp, M. Hattass, A. Czasch, L. P. H. Schmidt, and O. Jagutzki *accepted for publication in Radiation Physics and Chemistry* .
5. A. Kheifets and I. Bray *J. Phys.* **B31**, p. L447, 1998.
6. M. Pont and R. Shakeshaft *Phys. Rev.* **A51**, p. R2676, 1995.
7. L. Malegat, P. Selles, and A. Kazansky *Phys. Rev. Lett.* **85**, p. 21, 2000.
8. J. Colgan and M. S. Pindzola *Phys. Rev.* **A65**, p. 032729, 2002.
9. G. L. Kamta and A. F. Starace *Phys. Rev. Lett.* **86**, p. 5687, 2001.
10. A. Becker and F. Faisal *Phys. Rev.* **A50**, p. 3256, 1994.
11. B. Walker, B. Sheehy, L. DiMauro, P. Agostini, K. Schafer, and K. Kulander *Phys. Rev. Lett.* **73**, p. 1227, 1994.
12. T. Weber, M. Weckenbrock, A. S. and L. Spielberger, O. Jagutzki, V. M. and G. Urbasch, M. Vollmer, H. Giessen, and R. Dörner *Phys. Rev. Lett.* **84**, pp. 443, *J. Phys. B* **33** L127, 2000.
13. R. Moshhammer, B. Feuerstein, W. Schmitt, A. Dorn, C. Schröter, J. Ullrich, H. Rottke, C. Trump, M. Wittmann, G. Korn, K. Hoffmann, and W. Sandner *Phys. Rev. Lett.* **84**, p. 447, 2000.
14. R. Lafon, J. L. Chaloupka, B. Sheehy, P. M. P. P. Agostini, K.C.Kulander, , and L. F. DiMauro *Phys. Rev. Lett.* **86**, p. 2762, 2001.
15. E. Peterson and P. Bucksbaum *Phys. Rev.* **64**, p. 053405, 2001.
16. R. Moshhammer, J. Ullrich, B. Feuerstein, A. D. D. Fischer, C. D. Schröter, J. R. C. Lopez-Urrutia, C. Höhr, H. Rottke, C. Trump, M. Wittmann, G. Korn, K. Hoffmann, and W. Sandner *J. Phys* **B36**, p. L113, 2003.
17. T. Weber, H. Giessen, M. Weckenbrock, A. S. and L. Spielberger, O. Jagutzki, V. Mergel, G. Urbasch, M. Vollmer, and R. Dörner *Nature* **404**, p. 608, 2000.
18. B. Feuerstein, R. Moshhammer, D. Fischer, A. Dorn, C. D. S. J. Deipenwisch, J. Lopez-Urrutia, C. Höhr, P. N. J. Ullrich, H. Rottke, C. Trump, M. Wittmann, G. Korn, , and W. Sandner *Phys. Rev. Lett.* **87**, p. 043003, 2001.
19. M. Weckenbrock, A. Becker, A. Staudte, S. Kammer, M. Smolarski, V. R. Bhardwaj, D. M. Rayner, D. M. Villeneuve, P. B. Corkum, and R. Dörner *Phys. Rev. Lett.* **91**, p. 123004, 2003.
20. R. Dörner, T. Weber, M. Weckenbrock, A. Staudte, M. Hattass, H. Schmidt-Böcking, R. Moshhammer, and J. Ullrich *Advances in Atomic Molecular and Optical Physics* **48**(ed. B. Bederson, H. Walther), p. Academic Press, 2002.
21. M. Y. Kuchiev *Sov. Phys.-JETP Lett.* **45**, p. 404, 1987.
22. P. Corkum *Phys. Rev. Lett.* **71**, p. 1994, 1993.
23. A. Jaron and A. Becker *Phys. Rev.* **A67**, p. 35401, 2003.
24. M. Weckenbrock, D. Zeidler, A. Staudte, T. Weber, M. Schöffler, M. Meckel, S. Kammer, M. Smolarski, O. Jagutzki, V. R. Bhardwaj, D. M. Rayner, D. M. Villeneuve, P. B. Corkum, and R. Dörner *Phys. Rev. Lett.* **92**, p. 213002, 2004.
25. H. Niikura, F. Legare, R. Hasbani, M. Ivanov, D. Villeneuve, and P. Corkum *Nature* **417**, p. 917, 2002.
26. R. Panfili, S. Haan, and J. Eberly *Phys. Rev. Lett.* **89**, p. 113001, 2002.
27. T. Brabec, M. Ivanov, and P. Corkum *Phys. Rev. A* **54**, p. R2551, 1996.
28. R. Dörner, V. Mergel, O. Jagutzki, L. Spielberger, J. Ullrich, R. Moshhammer, and H. Schmidt-Böcking *Physics Reports* **330**, pp. 96–192, 2000.

29. J. Ullrich, R. Moshhammer, A. Dorn, R. D. and L. Ph. Schmidt, and H. Schmidt-Böcking *Rep. Prog. Phys.* **66**, p. 1463, 2003.
30. E. Eremina, X. Liu, H. Rottke, W. Sandner, A. Dreischuh, F. Lindner, F. Grasbon, G. Paulus, H. Walther, R. Moshhammer, B. Feuerstein, and J. Ullrich *J. Phys* **B36**, p. L311, 2003.
31. see Roentdek.com for details of the detectors.
32. M. Lewenstein, P. Balcou, M. Ivanov, A. L'Huillier, and P. Corkum *Phys. Rev. A* **49**, p. 2117, 1994.